Experimental transition probabilities for infrared lines of Cl I

J. M. Bridges and W. L. Wiese
National Institute of Standards and Technology, Gaithersburg, Maryland 20899, USA
(Received 29 October 2008; published 17 December 2008)

We operated a high-current, wall-stabilized arc in a gaseous mixture containing chlorine and observed 4*s*-4*p*, 4*p*-4*d*, and 4*p*-5*d* transitions in the red and near infrared spectrum. We measured their relative transition probabilities end-on and put them on an absolute scale with a lifetime value obtained from the literature. We achieved good agreement with recent sophisticated calculations and an earlier measurement for the stronger transitions, but encountered large differences for weak transitions.

DOI: 10.1103/PhysRevA.78.062508 PACS number(s): 32.70.Cs

INTRODUCTION

The transition probabilities of neutral chlorine have found a number of uses recently, since lines of the chlorine spectrum have been observed in fusion edge plasmas as well as in plasma etching steppers, due to the use of chlorine for cleaning purposes. Also, lines of neutral chlorine have been observed in interstellar space. Transition probability data are therefore needed for Cl impurity and abundance determinations. But experimental transition probability data for neutral chlorine are sparse, and the calculated results still show considerable scatter, especially for the weaker lines, despite the application of sophisticated multiconfiguration methods. Thus, additional experimental checks on the calculated data are desirable to reduce existing discrepancies. We have undertaken emission measurements of 4*s*-4*p*, 4*p*-4*d*, and 4*p*-5*d* lines in the visible and near infrared regions of the spectrum in order to improve the data situation.

EXPERIMENT

We used a wall-stabilized arc at a current of 40 A as our source for generating emission spectra of neutral chlorine under stable steady-state conditions. The arc column, about 100-mm long, was constricted and position stabilized by a stack of ten water-cooled copper disks with a central bore of 4 mm. The arc chamber was sealed from its surrounding atmosphere and kept just slightly above atmospheric pressure, and the electrode areas were operated in a mixture of argon and helium. In the central observation part, chlorine and oxygen were added to the mixture. The inclusion of helium resulted in a smaller underlying continuum intensity, permitting more accurate line intensity measurements. The oxygen admixture served for the determination of the plasma temperature from intensity measurements of oxygen lines of accurately known transition probabilities (A values), as described below. All gas flows were kept small, in the laminar range, and the chlorine was confined to the central part and prevented from entering the electrode areas by appropriate arrangement of the various gas flows and by positioning the gas exits some distance away from the electrodes. After exiting the arc, the gas passed through a scrubber to remove the chlorine and then passed through the laboratory exhaust system.

Since chlorine is corrosive to the copper plates, after a run of about 1–2 h the arc assembly had to be disassembled and cleaned of solid residue which had accumulated near the channel. Gradual drifts as well as significant fluctuations in the chlorine concentration initially made accurate intensity measurements difficult. Early on, we experimented with chloroform (CCl_4) to introduce chlorine into the arc chamber, but this did not lead to any improvement over chlorine gas. The stability was greatly improved by enlarging the centers of the copper disks and by inserting rings of nickel or graphite there. Graphite inserts were used for the three disks at the central part of the arc, and nickel inserts for the other disks closer to electrode regions. A slow drift of the chlorine concentration could not be eliminated, but was corrected for by continuously monitoring the intensity of a chlorine reference line and by adjusting the other chlorine line data according to the change observed for this line.

We observed the arc column end-on and focused its image onto the entrance slit of a 2 m monochromator equipped with either a 1200 lines per mm or 1800 lines per mm grating. Initially, a photomultiplier was used to obtain line intensity data, but it was replaced by a charge-coupled device (CCD) detector for subsequent measurements. The entrance slit of the monochromator was normally set at 20 μm. By using an aperture to restrict the beam to a small solid angle ($f/40$), only the approximately homogeneous high-temperature central area around the arc axial position was imaged on the slit. With a beam splitter and a small 0.5 m monochromator, the signal from a chlorine reference line was continuously monitored to insure accurate relative intensity measurements during extended runs, during which slow, but noticeable drifts occurred.

The presence of appreciable continuum radiation and the small drift in chlorine concentration during the runs limited the range of line intensities that could be accurately measured under a given set of conditions. The lines must be strong enough for making good intensity measurements but below the level at which significant self absorption occurs, since the determination of A values from emission measurements assumes negligible self-absorption. To obtain the best accuracy for all measured lines, the following procedure was used. First, the arc was operated with a concentration of chlorine appropriate for the strongest lines. After some runs in which the strongest lines were measured relative to each other, the flow rate of chlorine was increased to allow the measurement of additional weaker lines. Lines of intermediate intensity included in both sets of measurements served to normalize all measurements to a uniform relative scale. In

this manner, the relative intensities of the complete group of lines were determined. To insure that self-absorption was indeed negligible, the strongest lines in each run were checked by using a concave mirror behind the arc. This mirror reflected and re-focused the light coming out the rear of the arc back into the forward direction. Signals were measured both with and without this mirror included in the optical path, and from the ratio of these signals the amount of self-absorption can be calculated [1]. Actually, both the chlorine and oxygen concentrations were sufficiently limited in each run to keep self-absorption negligible.

Computer programs developed at the National Institute of Standards and Technology (NIST) were used for spectrometer control, data acquisition, and data analysis. After subtracting the continuum, the line profiles were fitted to a spline function which was then integrated to obtain the line intensities. A commercially available data analysis program was also used to deconvolute some spectral lines which were significantly blended with other lines. The individual line profiles were found to be well represented by Voigt functions. This allowed accurate intensity measurements of lines which are partially blended with other lines. As a consistency check, we determined the intensities of some isolated lines with a program developed in-house as well as with the commercial data analysis program, and achieved close agreement. A tungsten strip lamp calibrated by the Optical Technology Division of NIST was used as a radiometric standard to calibrate the response of the optical system as a function of wavelength. For each arc run, measurements of oxygen multiplets were included for determining the temperature of the arc plasma, as discussed below.

ANALYSIS

According to standard equilibrium criteria, the model of partial local thermodynamic equilibrium (PLTE) may be applied for the transitions of interest under our arc conditions [2]. This is primarily due to the relatively high electron density, which was measured from the widths of Stark broadened lines to be about 5×10^{22} m^{-3} in several earlier studies of our group under very similar conditions and with the same type of emission source. This allows us to put all our measurements from lines originating from various upper levels on a uniform relative scale, which we then convert to an absolute basis with a known radiative lifetime as discussed below. For plasmas in partial local thermodynamic equilibrium, relative intensities I(relative) of emitted spectral lines within an atomic species are proportional to

$$I(\text{relative}) \sim (g_m/\lambda)A \exp(-E_m/kT). \quad (1)$$

A is the transition probability for spontaneous emission, g_m is the statistical weight of the upper level m, E_m is the energy of the level, λ is the wavelength of the line, and k is the Boltzmann constant. This relation can thus be used to determine relative A values of measured lines if the plasma temperature T is known.

The plasma temperature can be determined by applying Eq. (1) to lines of known A values and by measuring their relative intensities. We chose oxygen lines for this purpose, in particular the multiplets at 777.3, 645.5, and 715.6 nm. In addition to their accurately known A values [3], the upper energy levels of these multiplets are widely separated from each other, resulting in an accurate local temperature determination using a "Boltzmann plot" [4]. For the arc runs in which line intensity measurements were made, the plasma temperature varied slightly for different gas mixtures, but for the area around the arc axis it always centered around 11 500 K within a band of ±100 K.

For each run in which data were obtained, the plasma temperature was determined from the oxygen line measurements, several chlorine lines were measured, and relative A values of these lines were calculated. Each line was measured three or more times relative to other lines, and the results were averaged. Finally, all measured lines were normalized to the same scale, using lines included in each of two separate runs for normalization. Relative A values were thus determined for a total of 33 chlorine lines.

The determination of absolute transition probabilities of the chlorine lines is possible if the number density of chlorine atoms (atoms per unit volume) can be determined. However, this is very difficult to achieve accurately for the gas mixture that we have utilized, since chlorine is but a small constituent, and "demixing" effects, which change the gas mixture ratio from its initial value, are known to occur in arc plasmas. However, an accurate absolute scale may also be determined from the measurement of the radiative lifetime of an appropriate Cl I energy level. Generally, the lifetime of a level is equal to the reciprocal of the sum of transition probabilities of all downward transitions from this level. Therefore measuring all lines emitted from a selected level will allow their relative transition probabilities to be normalized to absolute values. Among the energy levels of neutral chlorine whose lifetimes have been determined, the one most applicable for this work is $5d\ 2[4]_{9/2}$ measured by Delalic *et al.* [5] with the high-frequency deflection technique. This level is close to the ionization limit, and should be only slightly affected by cascades from higher levels, which could not be taken into account. From this level, according to spectroscopic ΔJ selection rules, only one relatively strong line is emitted. Therefore, its transition probability is to a good accuracy just the reciprocal of the level lifetime value. This line, at 639.866 nm, appeared broader and weaker than our other investigated lines, but by using higher concentrations of helium, its intensity was accurately measured relative to a few other lines, as previously discussed, and thereby included in the set of relative transition probabilities. The A values of all lines were then normalized to the value determined by the lifetime for the $5d\ 2[4]_{9/2}$ level.

RESULTS AND DISCUSSION

The absolute transition probabilities determined by this work are listed in Table I. The estimated combined standard uncertainty of all values is $\pm15\%$, except for the weakest line, where it is $\pm25\%$. This includes the estimated uncertainty in the lifetime determination ($\pm8\%$), as well as contributions from measurements of spectral line intensities, the temperature determination, and the radiometric calibration.

TABLE I. Transition probabilities (in 10^8 s^{-1}) and comparisons with other results. Our estimated combined standard uncertainty for all lines is ±15%, except for the weakest line at 855.044 nm, where it is ±25%, and the line at 639.866 nm where it is ±8% [5].

		Experiments		Calculations	
Transition	Wavelength (nm)	This work	Bengtson *et al.* [7]	Fischer *et al.* [8]	Oliver and Hibbert [9]
$4s\ ^2P_{3/2}$-$4p\ ^4D^o_{3/2}$	974.4426	0.0167		0.006342	0.01082
$4s\ ^4P_{1/2}$-$4p\ ^4P^o_{3/2}$	970.2439	0.0551		0.05836	0.05916
$4s\ ^2P_{3/2}$-$4p\ ^2D^o_{5/2}$	959.222	0.1508		0.1721	0.2184
$4s\ ^4P_{3/2}$-$4p\ ^4P^o_{5/2}$	958.4801	0.0368		0.04041	0.03991
$4s\ ^2P_{1/2}$-$4p\ ^2P^o_{3/2}$	945.210	0.1338		0.0608	0.1411
$4s\ ^4P_{3/2}$-$4p\ ^4P^o_{3/2}$	939.3862	0.0410		0.04295	0.04254
$4s\ ^2P_{3/2}$-$4p\ ^2D^o_{3/2}$	928.886	0.1435		0.08765	0.1501
$4s\ ^2P_{1/2}$-$4p\ ^4S^o_{3/2}$	919.7596	0.0272		0.04045	0.01698
$4s\ ^4P_{3/2}$-$4p\ ^4P^o_{1/2}$	919.1731	0.2173		0.2496	0.2490
$4s\ ^2P_{1/2}$-$4p\ ^2S^o_{1/2}$	904.543	0.2644		0.2639×10^{-4}	0.2519
$4s\ ^2D_{5/2}$-$4p\ ^2F^o_{7/2}$	903.8982	0.2676			0.2874
$4s\ ^4P_{5/2}$-$4p\ ^4P^o_{3/2}$	894.806	0.1606		0.1778	0.1764
$4s\ ^2P_{3/2}$-$4p\ ^2P^o_{3/2}$	891.292	0.0766		0.1289	0.1044
$4s\ ^2P_{3/2}$-$4p\ ^4S^o_{3/2}$	868.626	0.0443	0.0389	0.05795	0.03369
$4s\ ^4P_{3/2}$-$4p\ ^4D^o_{5/2}$	858.597	0.1646	0.99	0.2045	0.2269
$4s\ ^4P_{1/2}$-$4p\ ^4D^o_{3/2}$	857.524	0.1345	0.114	0.1517	0.1453
$4s\ ^2P_{3/2}$-$4p\ ^2S^o_{1/2}$	855.044	0.0085	0.0188	0.2776	0.04424
$4s\ ^4P_{1/2}$-$4p\ ^4D^o_{1/2}$	842.825	0.2611	0.190	0.2999	0.2914
$4s\ ^4P_{3/2}$-$4p\ ^4D^o_{3/2}$	833.331	0.1371	0.089	0.1523	0.1530
$4s\ ^4P_{1/2}$-$4p\ ^2D^o_{3/2}$	822.045	0.0313		0.01769	0.02049
$4s\ ^4P_{5/2}$-$4p\ ^4D^o_{5/2}$	821.204	0.0344	0.055	0.04307	0.04555
$4s\ ^4P_{3/2}$-$4p\ ^4D^o_{1/2}$	819.442	0.0328	0.042	0.03619	0.03546
$4s\ ^4P_{3/2}$-$4p\ ^2D^o_{3/2}$	799.785	0.0100	0.0209	0.01135	0.007653
$4s\ ^4P_{1/2}$-$4p\ ^2P^o_{3/2}$	792.4645	0.0151	0.021	0.03818	0.01104
$4s\ ^4P_{5/2}$-$4p\ ^2D^o_{5/2}$	787.822	0.0146	0.0179	0.01386	0.008751
$4p\ ^4P^o_{3/2}$-$4d\ 2[2]_{3/2}$	783.075	0.0716	0.097		0.05428
$4p\ ^4P^o_{5/2}$-$4d\ 2[3]_{7/2}$	782.136	0.1152	0.098		0.08459
$4s\ ^4P_{1/2}$-$4p\ ^4S^o_{3/2}$	774.497	0.0792	0.063	0.06211	0.07912
$4s\ ^4P_{3/2}$-$4p\ ^2P^o_{3/2}$	771.7581	0.0363	0.030	0.05520	0.02398
$4s\ ^4P_{3/2}$-$4p\ ^4S^o_{3/2}$	754.7072	0.1006	0.120	0.09979	0.1160
$4s\ ^4P_{5/2}$-$4p\ ^2P^o_{3/2}$	741.411	0.0392	0.047	0.06138	0.02578
$4s\ ^4P_{5/2}$-$4p\ ^4S^o_{3/2}$	725.662	0.1168	0.152	0.1145	0.1318
$4p\ ^4D^o_{7/2}$-$5d\ 2[4]_{9/2}$	639.866	0.0403			

In addition, the lifetime result probably contains a small systematic error due to cascading effects (not included). But the level used is highly excited and with a large J value and thus not subject to significant cascading. Indeed, the comparisons with other results in Table I indicate that this systematic error is at most at the 10% level. The wavelengths and line identifications were obtained from the NIST Atomic Spectra Database [6].

For comparison, the numbers from a previous experiment [7], and from the two most recent as well as most extensive multiconfiguration calculations [8,9] are also included in this table. The theoretical results are available both for the electric dipole length and for the electric dipole velocity approximations, but we have only used the dipole length results, as recommended by the authors. We also show graphical comparisons of our results with these data in Figs. 1–3.

Figure 1 illustrates that our values agree well with those of the 1971 emission measurements of Bengtson *et al.* [7], the only other experimental data for these lines. Their work was carried out with a gas-driven shock tube, and a state of local thermodynamic equilibrium was ascertained by several independent spectroscopic diagnostic techniques, so that absolute transition probabilities, without recourse to lifetime data, could be directly obtained. Most of their data agree

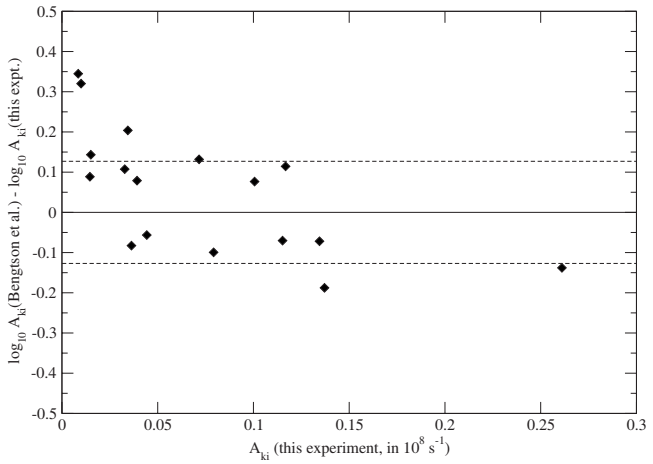

FIG. 1. Comparison of the measurements of Bengtson *et al.* [7] with this work. The $\log_{10}$ of the ratios of the transition probabilities are plotted versus our transition probability data. The line at 858.597 nm, an outlier, is omitted. The broken lines indicate the band of the combined uncertainties of ±34% (for the majority of the lines) around a perfect ratio of 1.00.

with our results within the combined estimated uncertainties of the two experiments, which are ±34% for most lines, but jump to ±52% for the weakest line at 855.044 nm. The uncertainties estimated by Bengtson *et al.* [7] are about twice as large as ours due mainly to their less precise photographic recording technique and their calibration of absolute line intensities. Since we normalize our values with a lifetime value, we require only the simpler determination of relative line intensities.

On the theoretical side, several advanced calculations were performed in recent years. We list in Table I the dipole length results of the two most recent works, which are also the most extensive multiconfiguration calculations for this spectrum, and present graphical comparisons with our measurements in Figs. 2 and 3. Froese Fischer *et al.* [8] used the

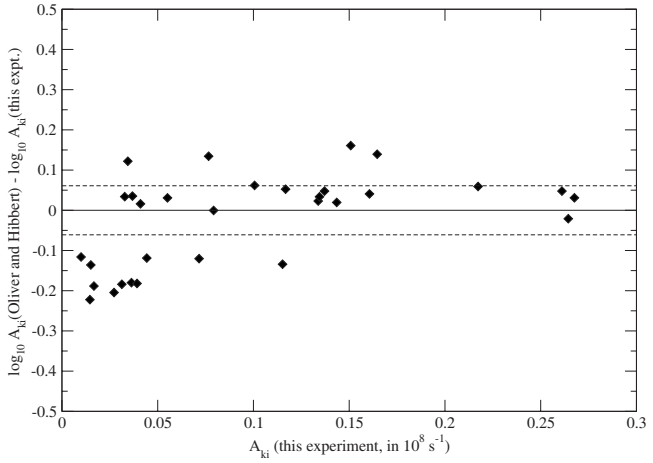

FIG. 2. Comparison of the results of the CIV3 calculations of Oliver and Hibbert [9] with this work. The $\log_{10}$ of the ratios of the transition probabilities are plotted versus our data. The line at 855.044 nm, an outlier, is omitted. The broken lines indicate the band of our uncertainties of ±15% around a perfect ratio of 1.00.

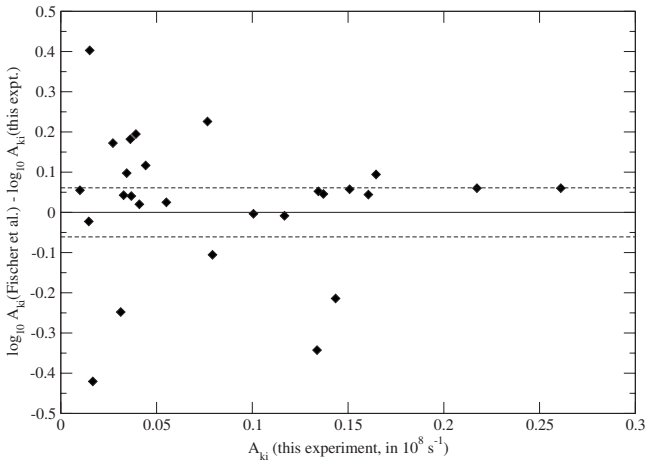

FIG. 3. Comparison of the results of the MCHF calculations of Froese Fischer *et al.* [8] with this work. The $\log_{10}$ of the ratios of the transition probabilities are plotted versus our data. Two outlying data points at 904.543 and 855.044 nm are omitted. The broken lines indicate the band of our uncertainties of ±15% around a perfect ratio of 1.00.

multiconfiguration Hartree-Fock (MCHF) method, with large expansions of the wave functions, up to 25 380 configuration state functions (CSFs). Oliver and Hibbert [9] carried out their calculations with the atomic structure code CIV3, expanding their wave functions into even larger sets of CSFs. For the comparisons with our measurements, it is appropriate to distinguish between the stronger lines, with A values greater than 10^7 s^{-1}, and the weaker lines. For the stronger lines, the values from this experiment are on average about 12% smaller than the calculated values, and the scatter of the ratios of our measured values with the calculated data is usually quite small, but with two (different) exceptions for each calculation. For many of these transitions, the differences between the calculated dipole length and dipole velocity results are only a few percent.

For the weaker lines the scatter between our experimental results and the calculated data increases strongly, to 50% and even more for a few values of Froese Fischer *et al.* [8]. For these transitions, the differences between the dipole length and dipole velocity results for the transition integral are also quite large, indicating increased uncertainties for the calculations. Significant cancellations of positive and negative terms in the transition integral are most likely responsible for this.

Earlier theoretical work for the Cl I spectrum was done with the CIV3 code by Ojha and Hibbert [10] and by Singh *et al.* [11], but with more limited configuration expansions of the wave functions. Their results show more scatter with our experiment and many larger differences between their dipole length and velocity data. Also, Lavin *et al.* [12] performed calculations with the relativistic quantum defect orbital (RQDO) method that disagree substantially with the above discussed more sophisticated calculations [8,9] and our measurements. We have therefore not included this earlier work in our general comparison table and graphs.

The situation for the $4s\ ^2P$-$4p\ ^2S$ doublet is quite interesting and deserves some special remarks. For this doublet we

TABLE II. Transition probabilities (in 10^8 s^{-1}) for the $4s\ ^2P$-$4p\ ^2S$ doublet.

	Experiment		Calculations							
Transition	Wavelength λ (nm)	This work	Ojha and Hibbert [10]	$d(l-v)$	Singh *et al.* [11]	$d(l-v)$	Oliver and Hibbert [9]	$d(l-v)$	Fischer *et al.* [8]	$d(l-v)$
$4s\ ^2P_{1/2}$-$4p\ ^2S_{1/2}$	904.543	0.2644 ±15%	0.2865	11.9%	0.1852	51.3%	0.2519	3.0%	0.2639E−04	96.9%
$4s\ ^2P_{3/2}$-$4p\ ^2S_{1/2}$	855.044	0.0085 ±25%	0.0177	17.3%	0.1621	11.4%	0.04424	18.3%	0.2776	8.2%

show in Table II our data, and four sets of recent theoretical results [8–11]. The table shows that the calculations and the measurements have produced widely different results for the weak line at 855.044 nm. For the strong transition at 904.543 nm, two of the four theoretical results are, within our uncertainty estimate, in agreement with our experimental value, while the third is 30% smaller, and in the MCHF calculation the labeling of the two transitions in the doublet appears to be reversed. However, for the weak transition, only the two experimental results agree within their rather large estimated uncertainties (see Table I), and all calculated data disagree with our result, two quite drastically.

For the $4s\ ^2P$-$4p\ ^2S$ doublet we have included in Table II the recent CIV3 calculations by Ojha and Hibbert [10] and Singh *et al.* [11] for the principal reason that these authors also include dipole length as well as dipole velocity results. Thus for all theoretical data the "length-velocity" (l-v) difference, which has been suggested as indicator of the level of accuracy of the calculated numbers [9,13], has been listed. The small l-v difference for the strong 904.543 nm line by Oliver and Hibbert shows that their two results have closely converged and should thus be of high accuracy. They are indeed closest to our measurement. However, this doublet case also shows that the l-v indicator does not work for the weak 855.044 nm transition. For this line similar length-velocity differences are obtained by the four authors, but the results are widely different, and none is close to our experimental number. Probably strong cancellation in the transition integral is responsible for the discrepancies, and since this is often the case for weak lines, the l-v indicator is not reliable for these.

In summary, the aim of this paper is to contribute to improving the data situation for the transition probabilities of neutral chlorine by providing fairly accurate experimental data for the persistent $4s$-$4p$ lines in the visible and near infrared spectrum. Our results show that the recent sophisticated multiconfiguration calculations [8,9], which have provided much larger sets of transition probabilities than this experiment, are expected to produce reliable data for lines of moderate and high strengths. As usual for such complex calculations, they do not provide explicit uncertainty estimates. But comparisons with our measurements show that for the stronger lines the differences between the dipole length and velocity results are generally good indicators of accuracy. For the weaker lines, however, these l-v differences do not provide reliable guidance, and factors such as partial cancellation in the transition integral should become more important. As seen in Figs. 2 and 3 and in the tables, the scatter between experiment and theory as well as between different advanced calculations increases substantially for the weak lines, leaving there a still unsatisfactory situation.

[1] V. Helbig, D. E. Kelleher, and W. L. Wiese, Phys. Rev. A **14**, 1082 (1976).
[2] H. R. Griem, *Principles of Plasma Spectroscopy* (Cambridge University Press, Cambridge, UK, 1997).
[3] W. L. Wiese, J. R. Fuhr, and T. M. Deters, J. Phys. Chem. Ref. Data, Monograph **7**, 335 (1996).
[4] J. M. Bridges and W. L. Wiese, Phys. Rev. A **57**, 4960 (1998).
[5] Z. Delalic, P. Erman, E. Kallne, and K. D. Zastrow, J. Phys. B **23**, 2727 (1990).
[6] NIST Atomic Spectra Database (Version 3.1.5), http://physics.nist.gov/asd3
[7] R. D. Bengtson, M. H. Miller, D. W. Koopman, and T. D. Wilkerson, Phys. Rev. A **3**, 16 (1971).
[8] C. F. Fischer, G. Tachiev, and A. Irimia, At. Data Nucl. Data Tables **92**, 607 (2006).
[9] P. Oliver and A. Hibbert, J. Phys. B **40**, 2847 (2007).
[10] P. C. Ojha and A. Hibbert, Phys. Scr. **42**, 424 (1990).
[11] N. Singh, A. K. S. Jha, and M. Mohan, Eur. Phys. J. D **38**, 285 (2006).
[12] C. Lavin, A. M. Velasio, and I. Martin, Astron. Astrophys. **328**, 426 (1997).
[13] Ch. Froese Fischer, Phys. Scr., T (to be published).